

International Journal of Control Theory and Applications

ISSN : 0974-5572

© International Science Press

Volume 10 • Number 34 • 2017

Robust Generalized Inversion Control: An Application to Satellite Launch Vehicle Attitude Control

Uzair Ansari¹ and Abdulrahman H. Bajodah²

¹ Aeronautical Engineering Department, King AbdulAziz University, Jeddah, Saudi Arabia
E-mail: uzansari@hotmail.com; abajodah@kau.edu.sa

Abstract: This paper addresses the nonlinear attitude control problem of Satellite Launch Vehicle (SLV) by using the inversion based technique called Generalized Dynamic Inversion (GDI). In this approach, the time differential form of differential constraint equation is evaluated along the vehicle's attitude trajectories which encapsulate the control objectives and are inverted to acquire the reference trajectory realizing control law. The inversion is being executed by utilizing Moore–Penrose generalised inverse and the associated null space projection for under determined algebraic systems. The GDI control law consists of two noninterfering control actions i.e. particular and auxiliary. The particular part is responsible for stable attitude tracking and it works to impose the predefined constraint dynamics. In auxiliary part, a null control vector is designed in which linear gain matrix is designed using control Lyapunov function to ensure asymptotic stability of body rate dynamics. The singularity problem associated with GDI is solved by augmenting a dynamic scale factor in the involved Moore–Penrose generalized inverse. A sliding mode based control loop is integrated to make GDI law robust against parametric variations and external disturbances. The overall stability of the control system is guaranteed by utilizing positive definite Lyapunov energy function, for stable attitude tracking. Numerical simulations are conducted under perturbed flight conditions, on six degree of freedom simulator of four-stage SLV, developed in Simulink/MATLAB.

Keywords: Generalized dynamic inversion, Satellite launch vehicle, Lyapunov stability, Modeling and simulation, Null control vector and Dynamic scale factor.

1. INTRODUCTION

The attitude control problem of Satellite Launch Vehicles (SLVs) has been acquiring significant attention for the last three decades. The challenges related to the design of attitude control system of SLVs are complex nonlinear coupled dynamics, uncertainties in aerodynamic parameters and in mass properties and external disturbances. Several linear feedback control algorithms with gain scheduling are proposed in literature. These linear algorithms require different control gains at selected operating points along the flight. Moreover, the robustness issues are still not completely addressed by employing these linear control techniques because of expanded range of flight conditions and due to parameter and modeling uncertainties. These characteristics of classical control have made these algorithms time consuming, thus increase both time and cost of control system development.

To overcome the limitations associated with linear control techniques and the complexity of gain scheduling, several nonlinear control techniques have been developed for SLV flight control. Among these are back stepping[1], sliding mode control[2], fault-tolerant control [3, 4] intelligent control [5, 6]. Within the last decade, Nonlinear Dynamic Inversion (NDI) has become a popular control methodology for flight control design. In NDI, the system nonlinearities have been eliminated by means of feedback. The NDI control in turns allows incorporating well recognized and established linear control methods to yield effective system designs. Several amendments were made in basic NDI methodology in order to improve its robustness characteristics [7-9]. However in practice it is difficult to attain perfect cancellation of plant inherent dynamics because of uncertain and un-modeled dynamics of plant, which in turns affect the controller's performance [10]. In addition to that the large control efforts, useful nonlinearity cancellation and computational issue that arise because of square matrix inversion impose limitations on NDI for its application to complex nonlinear systems. On the other hand Sliding Mode Control (SMC) emerging as a frontrunner control technique which is very popular due to its inherent robustness characteristics against modeling uncertainties, un-modeled dynamics and disturbances.

The new inversion based control that extends NDI is GDI, which is based on inverting a prescribed dynamic constraint of the plant rather to invert the system itself. In GDI dynamic constraints are defined that contains the control objectives and are inverted using Moore-Penrose Generalized Inverse (MPGI) based Greville formula [11] to get the control variables that realize that dynamics. This methodology has been applied to variety of aerospace engineering problems [12-18].

In this paper Robust GDI (RGDI) is proposed for attitude control of SLV. In particular part of GDI, a prescribed asymptotically stable dynamics of the attitude angles errors from their reference values is defined and are inverted to get the control law using MPGI to steer the attitude angles towards the generated reference profiles. In auxiliary part, null control vector is designed via control Lyapunov function to ensure asymptotic stability of inner body rate dynamics. For singularity avoidance, dynamic scale factor is introduced within MPGI in particular part of GDI for stable attitude tracking. Since GDI is explicitly based on mathematical model, an additional SMC element is incorporated in GDI control loop which provides robustness against modeling uncertainties and bounded external disturbances. A positive definite Lyapunov function is used to guarantee the overall stability of RGDI control methodology. To attain orbital parameters, external guidance loop is incorporated to generate the reshaped pitch and yaw attitude profiles based on positional errors in normal and lateral directions respectively. For performance evaluation, a detailed six Degree Of Freedom (DOF) nonlinear model of four-stage SLV is developed in Simulink/Matlab. Numerical simulations are conducted in perturbed flight conditions to show the efficacy of proposed control and guidance algorithm.

This paper is organized as follows. The SLV data and its reference trajectories are presented in section 2. The detailed modeling of kinematical and dynamical behaviour of SLV in Launch frame is discussed in section 3. The basic formulation of GDI control is presented in section 4. The singularity avoidance by augmenting dynamic scale factor is discussed in section 5. The design of null control vector for body rates stabilization using control Lyapunov function is presented in section 6. The design of RGDI by augmenting SMC based robust term is discussed in section 7 and the stability analysis of RGDI methodology is explained in section 8. The guidance algorithm is presented in section 9. Finally simulation results and conclusion are discussed in section 10 and 11 respectively.

2. SLV DATA AND REFERENCE TRAJECTORIES

To examine the performance of RGDI control with guidance for ascent flight phase, a data of four-stage launch vehicle is used [19] whose data is given in Table 1.

Table 1
Four-stage SLV data

Parameters	Stage-1	Stage-2	Stage-3	Stage-4
Stage mass (kg)	11836.87	4701.7	2436.65	459.73
Stage length (m)	5.178	2.089	2.047	4.29
Maximum control deflection (deg)	10.2	4	4	4
Stage burn time (s)	63	69	63.6	61.8

The flight trajectory consists of four burning phases along with two coasting phases after second and third stage burnout. The vehicle has the capability to inject the payload in circular Low Earth Orbit (LEO) having altitude of 300 km. The control maneuvering to track the desired roll, pitch and yaw attitude profiles is achieved by using four vernier motors, in which nozzles 2 and 4 are used for pitch, 1 and 3 for yaw and all four for roll. The reference trajectories for SLV were already simulated by using point mass model and are presented in [5]. The planar motion of vehicle is shown in Figure 1.

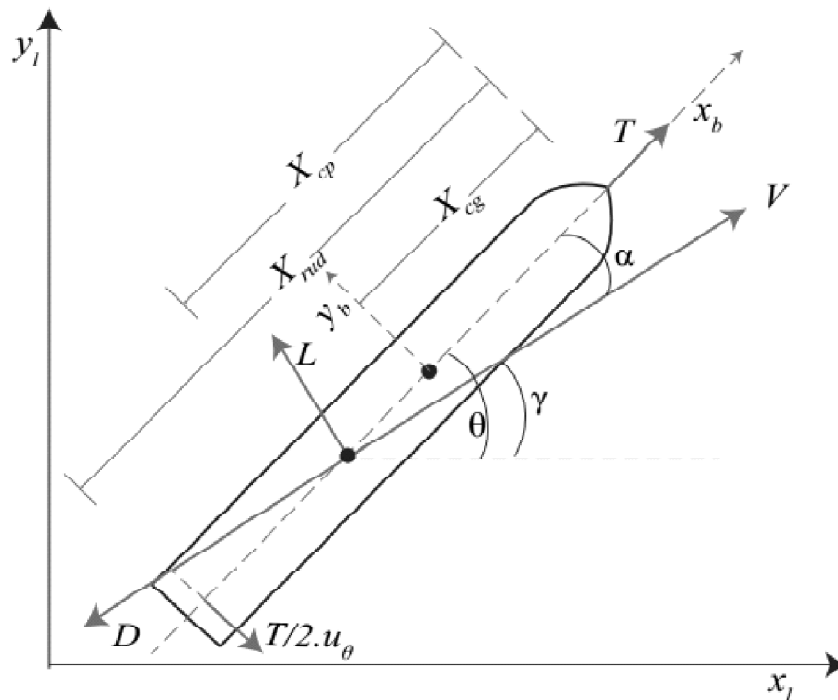


Figure 1: SLV planar motion symbol definition

In point mass model, the Angle of Attack and Side Slip attitude profiles are optimized offline using Genetic Algorithm. During optimization the structural constraints are put into consideration by confining aerodynamic loading and heating, especially for maneuvering in denser atmosphere. The reference trajectories after optimization are shown in Figure 2.

3. SIX DOF MATHEMATICAL MODELING OF SLV

To analyse the ascent flight, it is necessary to develop the kinematic and dynamic model of SLV. In mathematical modeling, the Earth is approximated to be an ellipsoid, and the axis passing through the north and south poles is

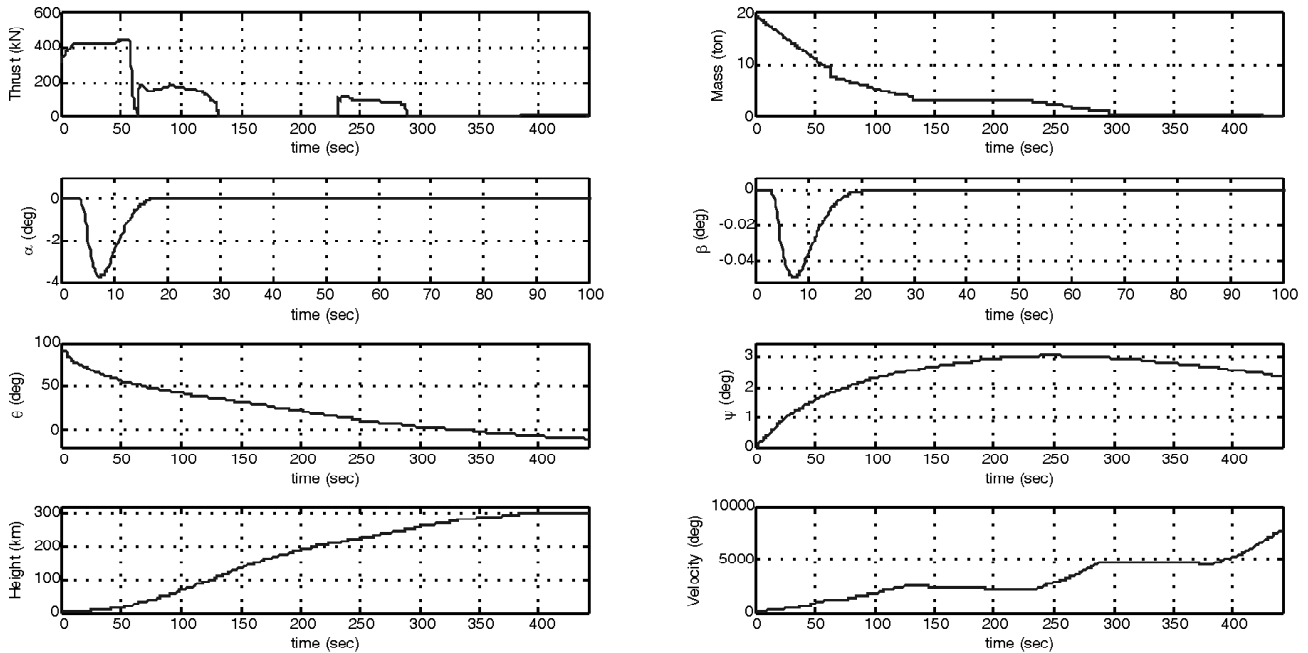


Figure 2: Launch Vehicle reference profiles

considered to be an axis of symmetry and an axis of rotation. The interaction between the earth and the SLV is modeled according to the two-body problem formulation, i.e. by ignoring the gravitational forces due to any other planets or stars. The effect of Earth's rotation is also considered by implementing Coriolis and centrifugal accelerations. The six DOF equations of motion in the Launch frame are given as [20]

$$\dot{x}_l = V_{xl} \quad (1)$$

$$\dot{y}_l = V_{yl} \quad (2)$$

$$\dot{z}_l = V_{zl} \quad (3)$$

$$\dot{\phi} = p + q \tan \psi \sin \phi + r \cos \phi \tan \psi \quad (4)$$

$$\dot{\theta} = q \sin \phi / \cos \psi + r \cos \phi / \cos \psi \quad (5)$$

$$\dot{\psi} = q \cos \phi - r \sin \phi \quad (6)$$

$$\begin{bmatrix} \dot{V}_{xl} \\ \dot{V}_{yl} \\ \dot{V}_{zl} \end{bmatrix} = \frac{1}{m} L_{lb} \begin{bmatrix} -QSC_D + T \cos \delta_\phi \\ QSC_{l\alpha} \alpha + 0.5T \cos \delta_\theta \\ QSC_{l\beta} \beta - T \cos \delta_\psi \end{bmatrix} + L_{le} \begin{bmatrix} g_{xe} \\ g_{ye} \\ g_{ze} \end{bmatrix} - L_{le} \begin{bmatrix} 0 \\ 0 \\ \omega_e \end{bmatrix}^X \begin{bmatrix} 0 \\ 0 \\ \omega_e \end{bmatrix}^X \begin{bmatrix} x_e \\ y_e \\ z_e \end{bmatrix} - L_{le} \begin{bmatrix} 0 \\ 0 \\ \omega_e \end{bmatrix}^X \begin{bmatrix} V_{xe} \\ V_{ye} \\ V_{ze} \end{bmatrix} \quad (7)$$

$$\dot{p} = M_x / J_x \quad (8)$$

$$\dot{q} = (J_z - J_x)pr / J_y + M_y / J_y \quad (9)$$

$$\dot{r} = -(J_y - J_x)pq/J_z + M_z/J_z \quad (10)$$

$$\theta = \gamma + \alpha, \quad \psi = \sigma + \beta. \quad (11)$$

In kinematical and dynamical equations, ϕ, θ, ψ represent Euler's roll, pitch and yaw angles respectively. The flight path and heading angles are shown by γ and σ , T is the total thrust, Q is dynamic pressure, ω_e is earth rotational speed with respect to inertial frame, S is the body cross sectional area, C_D is drag coefficient, Cl_α and Cl_β are lift coefficient derivatives with respect to α and β respectively, L_{lb} and L_{le} are body to launch and earth to launch frame transformation matrices respectively. The vectors $X_e = [x_e y_e z_e]^T, V_e = [V_{xe} V_{ye} V_{ze}]^T$, and $g_e = [g_{xe} g_{ye} g_{ze}]^T$ are the position, velocity, and acceleration-due-to-gravity vectors respectively, all expressed in the earth frame, whereas $V_l = [V_{xl} V_{yl} V_{zl}]^T$ is the velocity vector, expressed in the launch frame. The body roll, pitch, and yaw rate components relative to the inertial frame and expressed in the body frame are denoted by p, q , and r . The axes of the body frame in which the equations of motion were derived are chosen to be the principal body axes of the SLV, and the corresponding principal moments of inertia are J_x, J_y , and J_z respectively. In equations (9), (10) and (11), M_x, M_y , and M_z are the external roll, yaw, and pitch moments respectively, and are expressed as [20]

$$M_x = T b_{rud} \delta_\phi \quad (12)$$

$$M_y = Q S C_{L\beta} \beta (X_{cp} - X_{cg}) + 0.5T (X_{rud} - X_{cg}) \delta_\psi \quad (13)$$

$$M_z = -Q S C_{L\alpha} \alpha (X_{cp} - X_{cg}) + 0.5T (X_{rud} - X_{cg}) \delta_\theta \quad (14)$$

where b_{rud} is the distance between the center of the motor and the rocket's longitudinal axis, X_{cg} is the horizontal distance from the SLV's nose to its center of mass, X_{cp} is the horizontal distance from the SLV's nose to the center of pressure, and X_{rud} is the horizontal distance from the SLV's nose to the motor's hinge line. The aerodynamic coefficients in equations (13) and (14) have been generated by DATCOM throughout the flight envelop. The state vector of the launch vehicle is given by $X = [\phi \theta \psi p q r]^T$, and the control vector is $U = [\delta_\phi \delta_\theta \delta_\psi]^T$, where $\delta_\phi, \delta_\theta$, and δ_ψ stands for control deflection in roll, pitch, and yaw channels, respectively.

4. ATTITUDE CONTROL USING GDI

The state vector of SLV is decomposed into attitude state vector and body rates state vector x_i defined as

$$x_u = [\phi \theta \psi]^T, \quad x_i = [p q r]^T \quad (15)$$

The differential equations of body Euler's angles represented by equations (4), (5) and (6) is written in compact form as

$$\dot{x}_u = H(x_u)x_i \quad (16)$$

where

$$H(x_u) = \begin{bmatrix} 1 & \tan \psi \sin \phi & \cos \phi \tan \psi \\ 0 & \sin \phi / \cos \psi & \cos \phi / \cos \psi \\ 0 & \cos \phi & -\sin \phi \end{bmatrix} \quad (17)$$

The body rate dynamics of SLV \dot{x}_i is given as

$$\dot{x}_i = J^{-1} S^\times(x_i) J x_i + J^{-1} M \quad (18)$$

where $S^\times(\omega)$ represents skew symmetric cross product matrix corresponding to x_i , M is the summation of all the moments acting on the SLV and J is the diagonal inertia matrix. By placing control and aerodynamic moments from equations (12), (13), and (14), \dot{x}_i is expanded as

$$\dot{x}_i = J^{-1}S^\times(x_i)Jx_i + J^{-1}QSf(\alpha, \beta) + J^{-1}GU \tag{19}$$

where

$$f(\alpha, \beta) = \begin{bmatrix} lC_{mx} \\ C_{l\beta}\beta(X_{cp} - X_{cg}) \\ -C_{l\alpha}\alpha(X_{cp} - X_{cg}) \end{bmatrix} \tag{20}$$

and

$$G = \begin{bmatrix} Tb_{rud} & 0 & 0 \\ 0 & 0.5T(X_{rud} - X_{cg}) & 0 \\ 0 & 0 & 0.5T(X_{rud} - X_{cg}) \end{bmatrix} \tag{21}$$

In compact form the body rate dynamics \dot{x}_i is written as

$$\dot{x}_i = A_i(x_u, x_i) + B_iU \tag{22}$$

where

$$A_i(x_u, x_i) = J^{-1}S^\times(x_i)Jx_i + J^{-1}QSf(\alpha, \beta) \tag{23}$$

and

$$B_i = J^{-1}G \text{ and } U = [\delta_\phi, \delta_\theta, \delta_\psi]^T \tag{24}$$

4.1. Formulation of Dynamic Constraint

The GDI control is constructed by defining the constraint dynamics of body attitude angles. To define the time differential constraint dynamics, the error vectors of body attitudes and inner body rates are defined as

$$e_u = x_u - x_{ud}, \quad e_i = x_i - x_{id} \tag{25}$$

where $x_{ud} = [\phi_d \theta_d \psi_d]^T$ and $x_{id} = [p_d q_d r_d]^T$ are bounded vectors. The weighted error norm of body attitude dynamics is expressed as (26) In equation

$$\begin{aligned} \chi_u &= \|e_u\|_w^2 = k_1(\phi - \phi_d)^2 + k_2(\theta - \theta_d)^2 + k_3(\psi - \psi_d)^2 \\ &= k_1e_\phi^2 + k_2e_\theta^2 + k_3e_\psi^2 \end{aligned} \tag{26}$$

In equation (26) for the error deviation function, $k_i, i = 1, 2, 3$ are positive constants, and the letter denotes the error of the corresponding body attitude from its reference value. Now linear time varying ordinary differential constraint equation has been formulated which is based on the error deviation function given by equation (26). The order of the constraint dynamic is the relative degree of the error deviation function. The equation takes the following form

$$\ddot{\chi}_u + c_1(t)\dot{\chi}_u + c_2(t)\chi_u = 0 \tag{27}$$

where c_1, c_2 are selected such that second order constraint dynamic is uniformly asymptotically stable. The first and second order time derivatives of error deviation function are calculated as

$$\dot{x}_u = 2e_u^T \text{diag}(k_1, k_2, k_3)(H(x_u)x_i - \dot{x}_{ud}) \quad (28)$$

and

$$\begin{aligned} \ddot{x}_u = 2e_u^T \text{diag}(k_1, k_2, k_3)\{H(x_u)(A_i + B_i U) + \dot{H}(x_u)x_i - \ddot{x}_{ud}\} \\ + 2(H(x_u)x_i - \dot{x}_{ud})^T \text{diag}(k_1, k_2, k_3)(H(x_u)x_i - \dot{x}_{ud}) \end{aligned} \quad (29)$$

The notation represents the diagonal matrix whose diagonal elements are given by k_i . The function $\dot{H}(x_u)$ is the element-wise differentiation of $H(x_u)$. By placing these time derivative in the constraint dynamic equation given by (27), its algebraic form yields

$$A(x_u, t)U = B(x_u, x_i, t) \quad (30)$$

where

$$A = [2e_u^T \text{diag}(k_1, k_2, k_3)H(x_u)B_i] \quad (31)$$

and

$$B = \begin{bmatrix} -2e_u^T \text{diag}(k_1, k_2, k_3)(-\ddot{x}_{ud} + \dot{H}(x_u)H(x_u)^{-1}x_{ud} + H(x_u)A_i \\ -2\dot{e}_u^T \text{diag}(k_1, k_2, k_3)\dot{e}_u - 2c_1 e_u^T \text{diag}(k_1, k_2, k_3)\dot{e}_u - c_2[k_1, k_2, k_3]\dot{e}_u \end{bmatrix} \quad (32)$$

Equation (30) is an under-determined algebraic system having infinite number of solutions. These solutions can be parameterized by generalized inversion using the Greville formula

$$U = A^+(x_u, t)B(x_u, x_i, t) + P(x_u, t)\zeta \quad (33)$$

where A^+ is the Moore-Penrose generalized inverse (MPGI), $\zeta \in \mathbb{R}^3$ is null control vector, and P is the null projection matrix given by

$$P(x_u, t) = I_{3 \times 3} - A^+(x_u, t)A(x_u, t) \quad (34)$$

Now substitute the control expression given by equation (33) in (22), the body rate dynamics is now written as

$$\dot{x}_i = A_i(x_u, x_i) + B_i\{A^+(x_u, t)B(x_u, x_i, t) + P(x_u, t)\zeta\} \quad (35)$$

The control law given by equation (33) enforces the uniform asymptotic stability of constraint dynamic given by equation (27); it also provides partial closed loop stability with respect to attitude dynamics given by equation (16). However, generalized inversion has its limitations when it is applied to matrices with variable elements due to the singularity problem. This problem arises when the inverted matrix tends to change rank, which causes discontinuity and causes the elements of the MPGI matrix to go unbounded. In this paper the inclusion of dynamic scale factor [16, 21] is utilized to tackle the problem of GDI singularity.

5. GDI SINGULARITY AVOIDANCE

A first order dynamic scale factor is integrated in MPGI to deal with the singularity issue associated with GDI, which is defined as

$$\dot{v}(t) = -v(t) + \frac{\gamma \|e_i(t)\|^2}{\|e_u(t)\|^2}, \quad v(0) > 0 \quad (36)$$

The first order differential equation given by (36) is asymptotically stable, wherein the forcing term is a positive real valued constant. Now the modified generalized inverse is written as

$$A^*(x_u, t) = A^T(x_u, t)\{A(x_u, t)A^T(x_u, t) + v(t)\}^{-1} \tag{37}$$

By employing the new definition of modified generalized inverse the GDI law becomes

$$U^* = A^*(x_u, t)B(x_u, x_i, t) + P(x_u, t)\zeta \tag{38}$$

Now closed loop body rate dynamics given by equation (35) becomes

$$\dot{x}_i = A_i(x_u, x_i) + B_i\{A^*(x_u, t)B(x_u, x_i, t) + P(x_u, t)\zeta\} \tag{39}$$

Theorem 1: Consider the closed loop system given by equations (16) and (39), and assume that $\|e_i(t)\| < \infty$ and that $\psi \neq 90$ for all $t \geq 0$, then the elements of A^* are bounded for all $t \geq 0$.

Proof: As time tends to infinity, the asymptotically stable first order dynamics given by equation (36) satisfies

$$\lim_{t \rightarrow \infty} v(t) = \lim_{t \rightarrow \infty} \frac{\gamma \|e_i(t)\|^2}{\|e_u(t)\|^2} \tag{40}$$

Hence

$$\lim_{t \rightarrow \infty} A^*(x_u, t) = \lim_{t \rightarrow \infty} A^T(x_u, t) \left\{ A(x_u, t)A^T(x_u, t) + \frac{\gamma \|e_i(t)\|^2}{\|e_u(t)\|^2} \right\}^{-1} \tag{41}$$

In equation(41), the inverse always exists if the right side of equation (40) is finite and non-zero since AA^T is non-negative definite. It remains to verify that the inverse exists for the two limit conditions

$$\lim_{t \rightarrow \infty} v(t) = \lim_{t \rightarrow \infty} \frac{\gamma \|e_i(t)\|^2}{\|e_u(t)\|^2} = \infty \tag{42}$$

$$\lim_{t \rightarrow \infty} v(t) = \lim_{t \rightarrow \infty} \frac{\gamma \|e_i(t)\|^2}{\|e_u(t)\|^2} = 0 \tag{43}$$

Considering that $\|e_i(t)\| < \infty$ and $\psi \neq 90$ for all $t \geq 0$, if the first limit condition given by equation (42) holds true then equation(41) implies that

$$\lim_{t \rightarrow \infty} A^*(x_u, t) = \lim_{t \rightarrow \infty} A^T(x_u, t)\{\infty\}^{-1} = 0_{3 \times 1} \tag{44}$$

If the second limit condition is satisfied then equation (41) implies that

$$\lim_{t \rightarrow \infty} A^*(x_u, t) = \lim_{t \rightarrow \infty} A^T(x_u, t)\{A(x_u, t)A^T(x_u, t)\}^{-1} = A^+(x_u, t) \tag{45}$$

Hence

$$\lim_{t \rightarrow \infty} (\|e_u(t)\|^2) = 0 \tag{46}$$

It is inferred from equation(46) that to satisfy equation(43), the following condition must be satisfied

$$\lim_{t \rightarrow \infty} (\|e_i(t)\|^2) = 0 \tag{47}$$

which implies that the error vectors e_u and e_i all converge to zero, proving that the elements of A^* are bounded and the constraints given by equation (27) is asymptotically stable

6. NULL CONTROL FOR BODY RATES STABILIZATION

The null control vector ζ is designed by using control Lyapunov function to guarantee global closed-loop stability of body rate dynamics. The null control vector is considered to be a linear function as

$$\zeta = Ke_i = K(x_i - x_{id}) \quad (48)$$

The value of the gain K is determined with the aid of a control Lyapunov function. By placing the value of ζ in equation (39), we get

$$\dot{x}_i = A_i(x_u, x_i) + B_i\{A^*(x_u, t)B(x_u, x_i, t) + P(x_u, t)Ke_i\} \quad (49)$$

The desired values of body rate dynamics are $x_{id} = 0_{1 \times 3}^T$. Now the desired body rate dynamics can be constructed by replacing x_i with x_{id} and \dot{x}_i with \dot{x}_{id} as

$$\dot{x}_{id} = A_i(x_u, x_{id}) + B_i\{A^*(x_u, t)B(x_u, x_{id}, t)\}. \quad (50)$$

By subtracting equation (50) from (49), the error dynamics is obtained as

$$\begin{aligned} \dot{e}_i = \dot{x}_i - \dot{x}_{id} = & A_i(x_u, x_i) - A_i(x_u, x_{id}) + B_i\{A^*(x_u, t)B(x_u, x_i, t) \\ & + P(x_u, t)Ke_i\} - B_i\{A^*(x_u, t)B(x_u, x_{id}, t)\}. \end{aligned} \quad (51)$$

In compact form the error dynamics given by equation (51) is written as

$$\dot{e}_i = \Delta_i(x_u, x_i, x_{id}) + B_iP(x_u, t)Ke_i \quad (52)$$

where

$$\begin{aligned} \Delta_i(x_u, x_i, x_{id}) = & A_i(x_u, x_i) - A_i(x_u, x_{id}) + B_iA^*(x_u, t)B(x_u, x_i, t) \\ & + B_iA^*(x_u, t)B(x_u, x_{id}, t) \end{aligned} \quad (53)$$

Consider the Lyapunov function

$$V_\zeta(x_u, t) = e_i^T \bar{P}(x_u, t)e_i \quad (54)$$

where the matrix $\bar{P}(x_u, t) = P + \varepsilon I_{3 \times 3}$ is positive symmetric definite, in which ε is an arbitrary positive real scalar. The derivative of the Lyapunov function given by equation (54) is written as

$$\dot{V}_\zeta(x_u, t) = 2e_i^T \bar{P}(\Delta + B_iPKe_i) + e_i^T \dot{\bar{P}}e_i = e_i^T (2\bar{P}\Delta + 2\bar{P}B_iPKe_i + \dot{\bar{P}}e_i). \quad (55)$$

In equation (55), $\dot{\bar{P}} = \dot{P}$ is the element-wise time derivative of \bar{P} . For global asymptotic stability of body rate dynamics we know that $\dot{V}_\zeta < 0 \forall e_i \neq 0$. This can be insured by the presence of symmetric positive definite matrix Q such that

$$\dot{V}_\zeta = -e_i^T Qe_i < 0 \quad (56)$$

Equating equation (55) with (56) yields

$$e_i^T (2\bar{P}\Delta + 2\bar{P}B_iPKe_i + \dot{\bar{P}}e_i + Qe_i) = 2\bar{P}\Delta + 2\bar{P}B_iPKe_i + \dot{\bar{P}}e_i + Qe_i = 0 \quad (57)$$

Multiplying equation (57) from the left by P^2 , and noticing the P is idempotent, i.e., $PP = P$, then the value of the projected gain PKe_i is solved for from equation (57) as

$$PKe_i = P\zeta = -(\bar{P}B_i)^{-1}P\left(\bar{P}\Delta + \frac{\dot{P}e_i}{2} + \frac{Qe_i}{2}\right) \quad (58)$$

If the projected null control vector $P\zeta$ given by (58) is applied, then it provides global partial asymptotic stability of the inner body rate dynamics. With this null control, the GDI based control law is given as

$$U^* = A^*B - P(\bar{P}B_i)^{-1}P\left(\bar{P}\Delta + \frac{\dot{P}e_i}{2} + \frac{Qe_i}{2}\right) \quad (59)$$

7. ROBUST GDI BASED ON SMC

The main purpose of the augmentation of SMC is to provide robustness against unknown but bounded disturbances and modeling uncertainties. A robust term is being included in the framework of GDI which yields

$$U^* = A^*(x_u, t)B(x_u, x_i, t) - P(x_u, t)\zeta - CA^*(x_u, t)\frac{S}{\|S\|} \quad (60)$$

where, $CA^*(x_u, t)\frac{S}{\|S\|}$ is the gain to enforce sliding, and S is the sliding surface for attitude dynamics defined as

$$S = \dot{\chi}_u + c_1(t)\chi_u + c_2 \int \chi_u \quad (61)$$

The control law given by equation (60) is capable of attracting the sliding surface given by equation (61), and enforcing the system trajectories to slide along the sliding surface. The derivative of the sliding surface is written as

$$\dot{S} = \ddot{\chi}_u + c_1(t)\dot{\chi}_u + c_2(t)\chi_u \quad (62)$$

By solving equation (27) and (62) we get

$$\dot{S} = A(x_u, t)U^* - B(x_u, x_i, t) \quad (63)$$

8. STABILITY ANALYSIS OF ROBUST GDI

To prove the stability of RGDI based attitude control system, we need to show that $S\dot{S} < 0$. The value of U^* given by equation (60) is placed in (63) which yields

$$\dot{S} = A(x_u, t)\left[A^*(x_u, t)B(x_u, x_i, t) - P(x_u, t)\zeta - CA^*(x_u, t)\frac{S}{\|S\|}\right] - B(x_u, x_i, t) \quad (64)$$

The expression of null projection matrix from equation (34) is placed in equation (64), we get

$$\begin{aligned} \dot{S} = & A(x_u, t)A^*(x_u, t)B(x_u, x_i, t) - A(x_u, t)I_{3 \times 3}\zeta + A(x_u, t)A^*(x_u, t)A(x_u, t)\zeta \\ & - CA(x_u, t)A^*(x_u, t)\frac{S}{\|S\|} - B(x_u, x_i, t) \end{aligned} \quad (65)$$

The delta commands for pitch and yaw axes represented by and respectively are computed as

$$\Delta_{\theta} = k_{\theta} E_y \quad (74)$$

$$\Delta_{\psi} = k_{\psi} E_z \quad (75)$$

where k_{θ} and k_{ψ} are the positive gains. The delta commands Δ_{θ} and Δ_{ψ} are added to the reference pitch and yaw profiles to produce the reshaped pitching Δ_r and yawing ψ_r attitude profiles. These reshaped profiles along with roll attitude ϕ_d are accurately tracked by RGDI based autopilot. This online reshaping brings the vehicle back to its desired path in perturbed flight conditions. An engine shutoff mechanism is implemented during the end of third stage powered phase for attaining the desired orbital velocity and altitude. The engine shutoff mechanism based on the magnitude of semi major axis a , which is calculated online and compared with reference value of a acquired at third stage burnout. As soon as it achieves the reference value of; thrust from the engine is cut off. The semi major axis a is defined as

$$a = \frac{r\mu}{2\mu - rV^2} \quad (76)$$

where $\mu = GM$, in which G is Gravitational constant, M is the mass of Earth and r is the position vector defined

$$\text{as } r = \sqrt{x_l^2 + (y_l + R_e)^2 + z_l^2}.$$

10. SIMULATION RESULTS

In this section, the performance of proposed control and guidance algorithm is evaluated on six DOF SLV simulator, in the presence of external disturbances and parametric variations. Numerical simulations are conducted for attitude tracking of SLV for the following two conditions

- Attitude tracking
- Robust analysis

10.1. Attitude Tracking

In this scenario, numerical simulation is conducted by considering thrust misalignment of 0.28 degree, in order to deviate the vehicle from its nominal path. Variation of 1% in thrust and 5% in drag are also considered. Wind profile is applied as external disturbance with maximum amplitude of 124 m/s with azimuth angle of 180 degree. The RGDI based controller performance is seen from Figure 4, in which it effectively tracks the desired roll, pitch and yaw attitude trajectories. The tracking is lost because of the un-powered flight phase, after second and third stage burnout. The online reshaped trajectory for pitch and yaw axes marked with black is being generated by external guidance loop, in order to minimize the positional errors in normal and lateral directions respectively.

The control commands generated for roll, pitch and yaw axes are shown in Figure 5. The control commands for roll, pitch, and yaw are zeros during the two coasting phases because of unavailability of thrust. Simulations demonstrate that the required control input magnitudes are realizable.

Angular body rates are shown in Figure 6. It is evident that the body rates are small throughout the ascent flight phase and do not involve high fluctuations, which implies that the control commands are sufficiently smooth. Such an advantage is important because the vehicle is inherently unstable, and fluctuating control commands cause the vehicle to experience high oscillations, especially in the high dynamic pressure region.

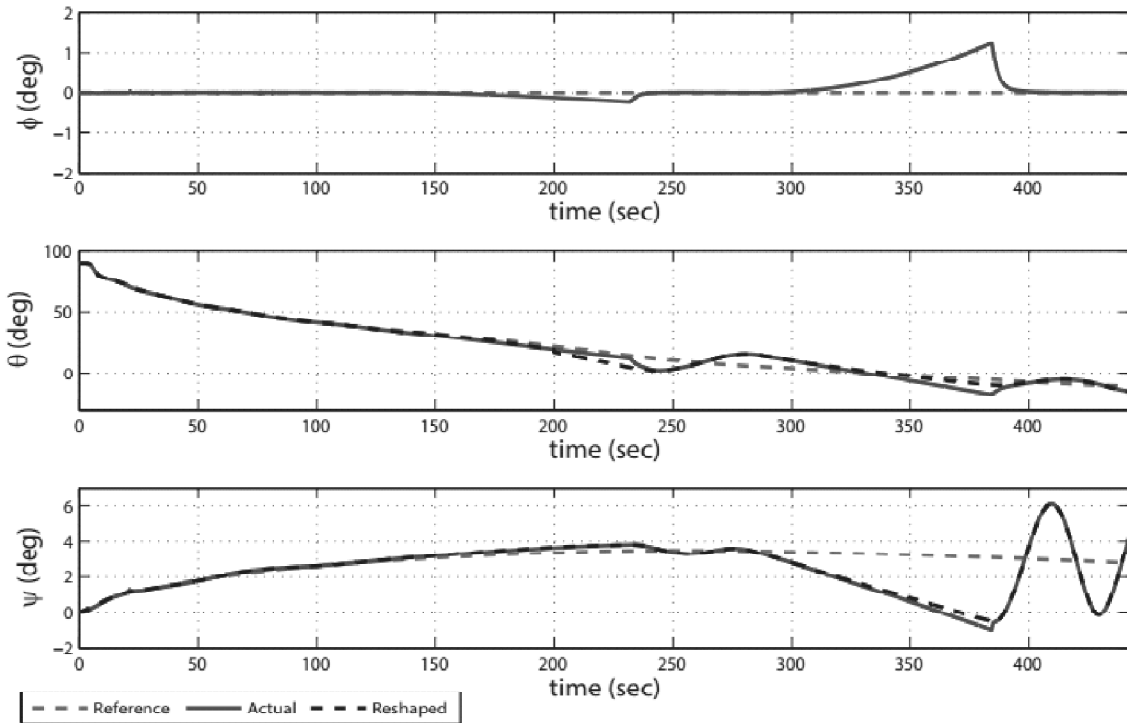


Figure 4: Attitude angles vs. time

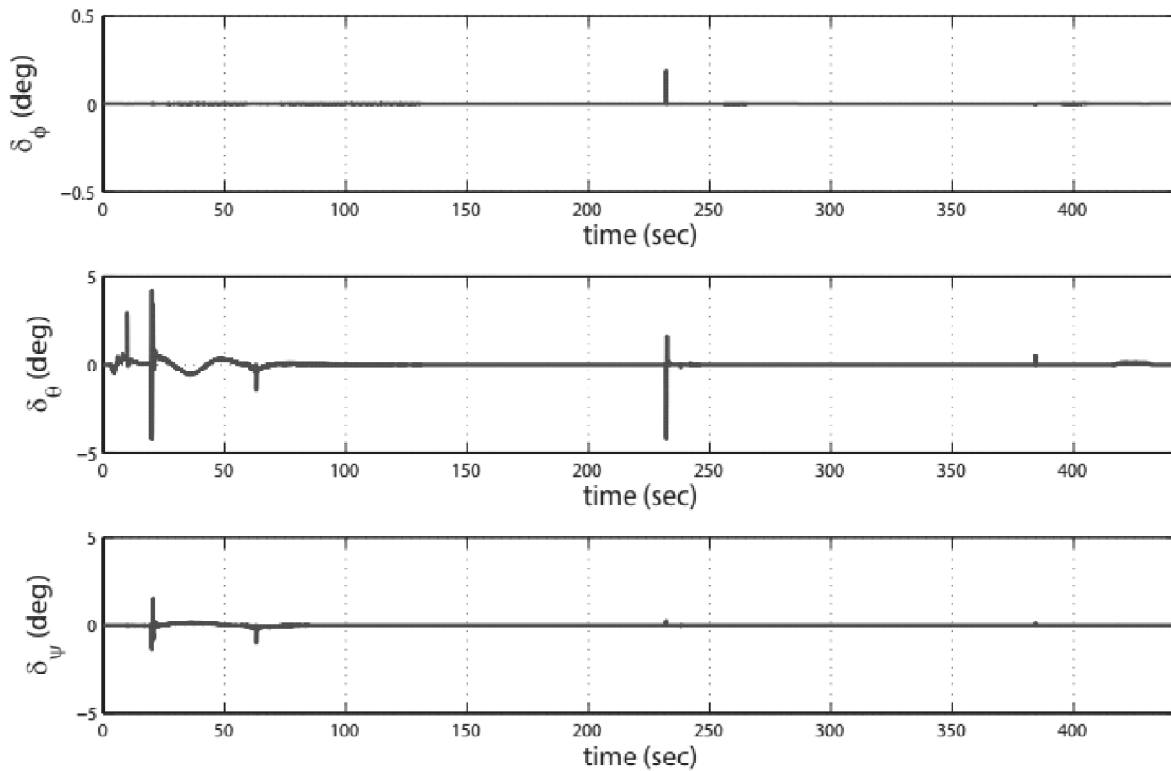


Figure 5: Control deflections vs. time

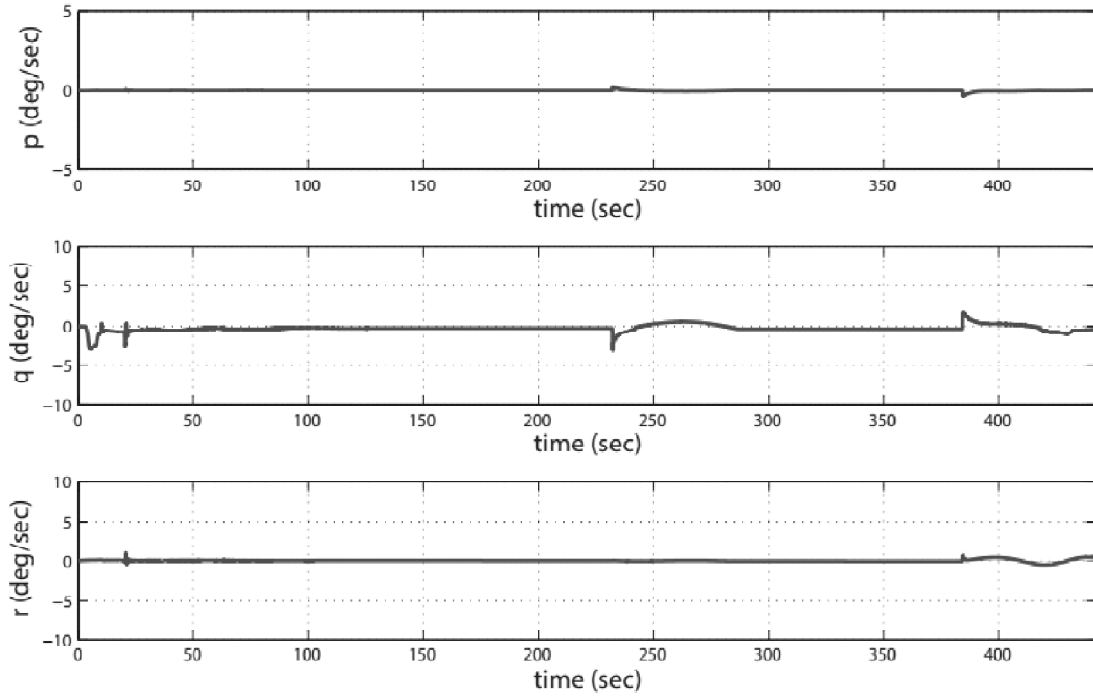


Figure 6: Body rates vs. time

The orbital height is shown in Figure 7, in which the results are being presented with and without guidance scheme, to visualize the magnitude of error generated by parametric variations and external disturbances. By inclusion of reshaped pitch and yaw attitude profiles and engine shutoff mechanism, the vehicle has successfully achieved the required circular orbit.

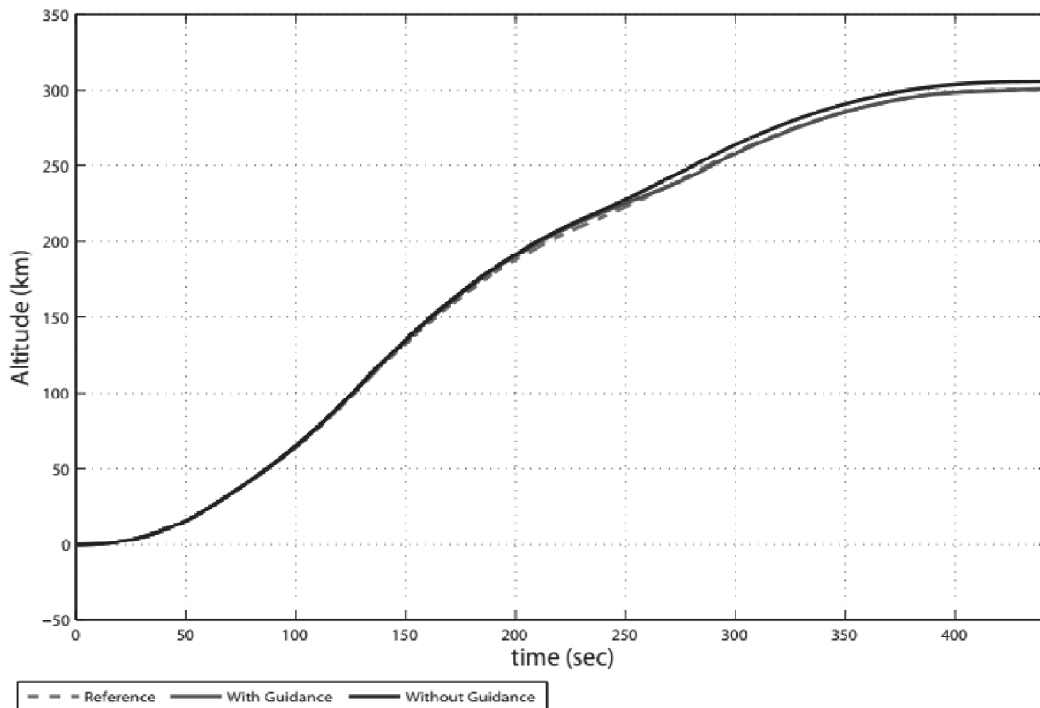


Figure 7: Altitude vs. time

10.2. Robust Analysis

To analyse the robustness of proposed guidance and control system, two cases are simulated in perturbed flight conditions with variations in aerodynamic coefficients and mass properties. The magnitude of external disturbances and parametric variations are shown in Table 2.

Table 2
Parametric variations

Parameters	Case-1	Case-2
I_{sp} Variation (%)	0.5	1.2
Thrust Misalignment (deg)	0.57	0.28
Drag Variation (%)	6.7	3
Variation in $C_{L\alpha}$, $C_{L\beta}$ (%)	10	5
X_{cp} Variation (%)	10	5
X_{cg} Variation (%)	10	5
Wind Azimuth (deg)	270	130

In presence of above listed disturbances and parametric variations, the proposed guidance and control performance for the two cases are shown in Figures 8-10.

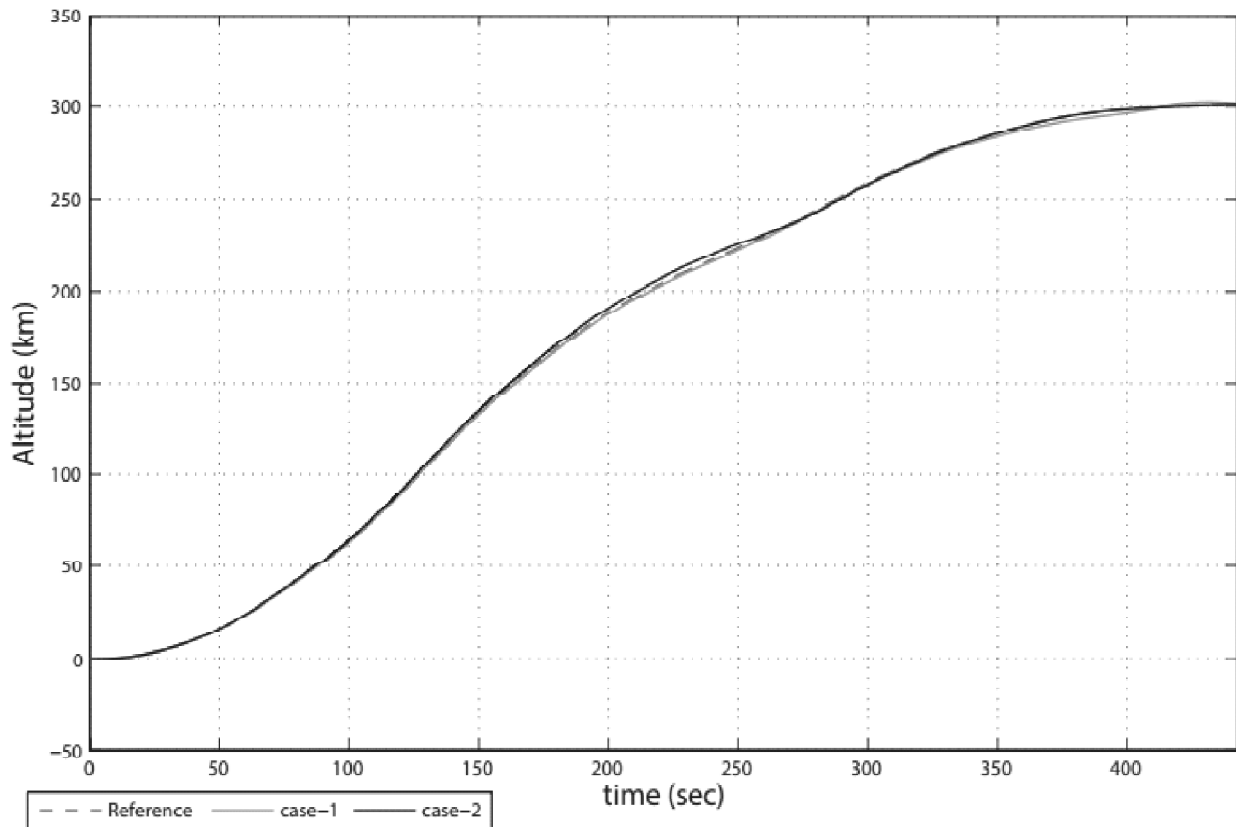


Figure 8: Altitude vs. time

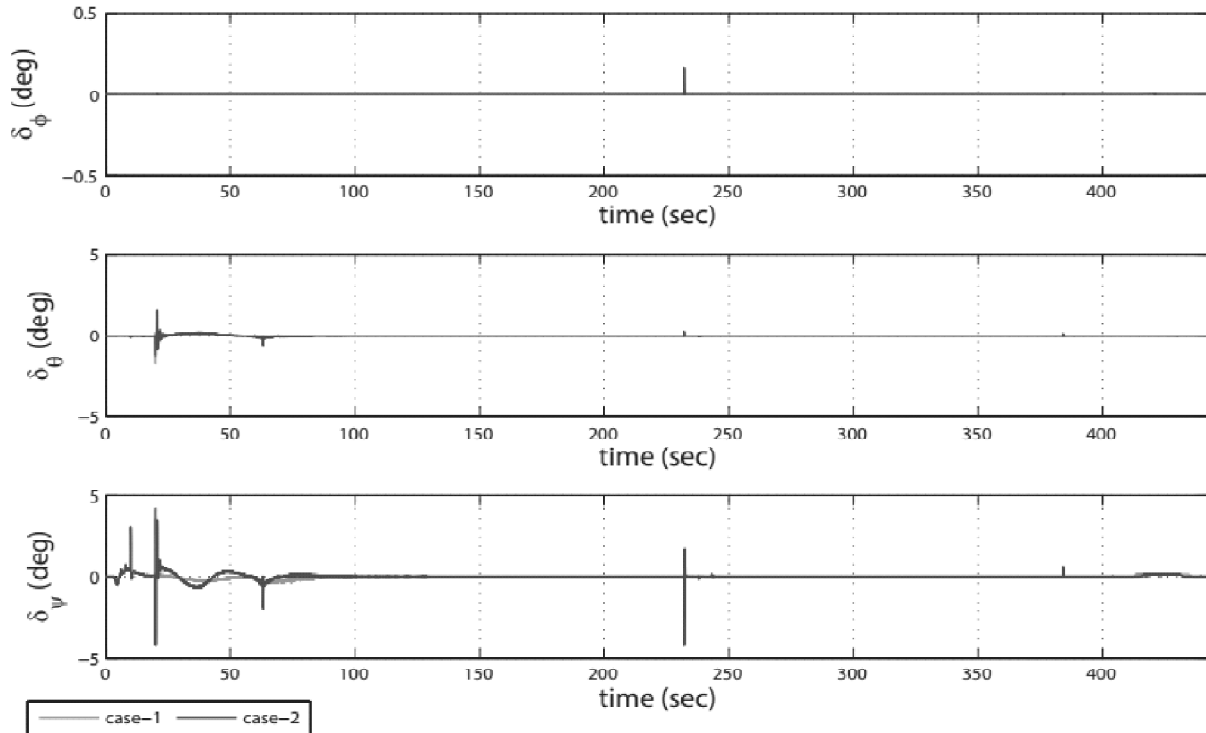


Figure 9: Control deflections vs. time

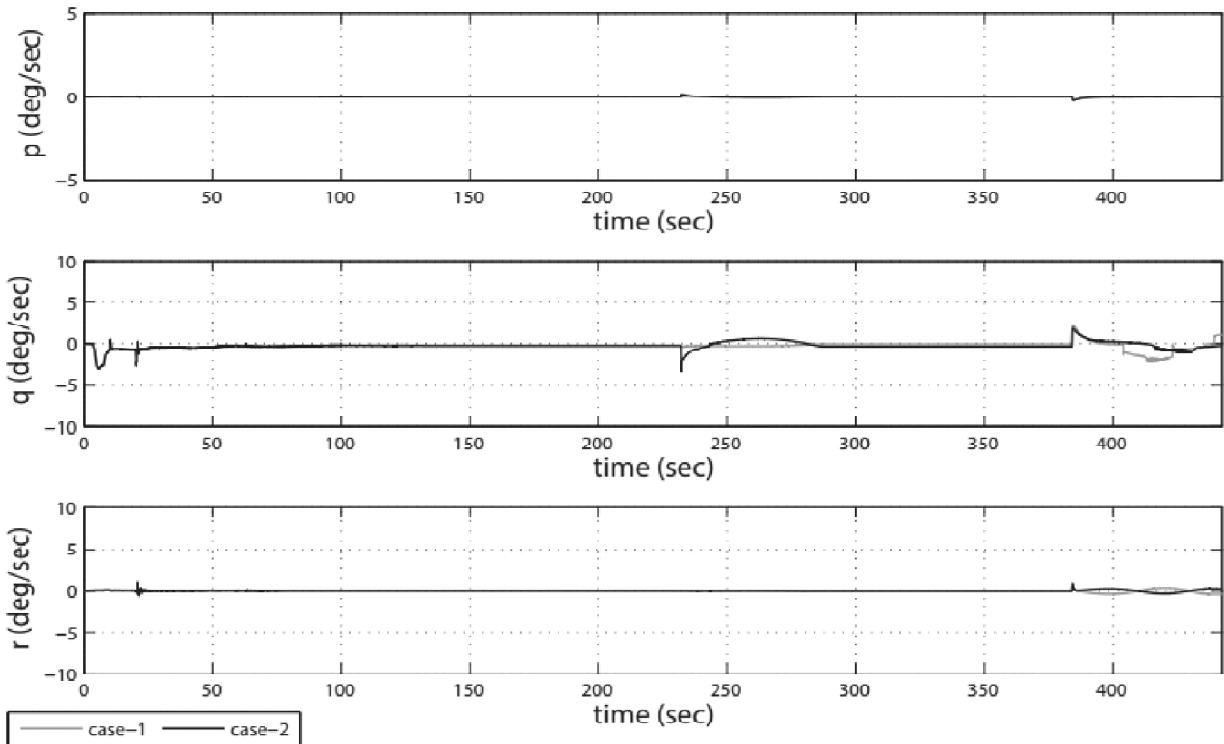


Figure 10: Body rates vs. time

The simulation results show the robust behaviour of trajectory following guidance and RGDI based autopilot against parametric uncertainties and external disturbances. It is apparent from the results that the proposed control law along with the guidance, effectively injects the satellite into the desired circular orbit as seen in Figure 8. The control commands and body rates for the two cases are shown in Figure 9 and 10 respectively, which clearly depicts the stable performance of proposed control and guidance law.

11. CONCLUSIONS

In this paper, a novel approach based on RGDI is presented for launch vehicle attitude control. To generate reference trajectories, the data of a four stage vehicle is used. In SIMULINK/MATLAB® environment, a detailed six DOF mathematical model is developed to simulate the ascent flight trajectory of the SLV. In GDI, dynamic constraint on the SLV attitude dynamics is defined and inverted by using the MPGI based Greville formula. The body rate dynamics is globally stabilized by means of the null control vector in the auxiliary part of the GDI control law, which is designed via a quadratic Lyapunov control function of the inner error variables. The generalized inversion singularity is avoided by augmenting a dynamic scaling factor in the MPGI that is involved in the particular part of the robust GDI control law. To make GDI robust against system nonlinearities, parametric variations and external disturbances, SMC-based robust term is augmented in the framework of GDI. For injection accuracy, trajectory following guidance is included in the outer loop, which reshapes the reference pitch and yaw attitude profile based on normal and lateral position errors respectively in real time. For performance evaluation, numerical simulations have been conducted in the presence of model uncertainties and external disturbances. Results of six DOF simulations exhibit the efficacy of designed control and guidance algorithm, which accurately track the required attitude profiles in perturbed flight conditions along with attaining desired orbital parameters.

REFERENCES

- [1] A. Steinicke and G. Michalka, "Improving transient performance of dynamic inversion missile autopilot by use of backstepping," *AIAA Guidance, Navigation, and Control Conference and Exhibit*, 2002.
- [2] Z. Wang, L. Liu, Y. Wang, and Z. Wang, "Dynamic integral sliding mode for launch vehicle Attitude control system," *Proc. 24th Chinese Control and Decision Conference, (CCDC)*, 1713–1718, 2012.
- [3] R. Das, S. Sen, and S. Dasgupta, "Fault tolerant controller for attitude control of satellite launch vehicle via LMI approach," *In. Proceedings of the First IEEE India Annual Conference*, 304–309, 2004.
- [4] R. Das, S. Sen, and S. Dasgupta, "Robust and fault tolerant controller for attitude control of a satellite launch vehicle," *IET Control theory & applications*, **1**(1), 304–312, 2007.
- [5] U. Ansari, S. Alam, and S. Minhaj un Nabi Jafri, "Trajectory optimization and adaptive fuzzy based launch vehicle attitude control," *In. 20th Mediterranean Conference on Control & Automation, MED*, 457–462, 2012.
- [6] U. Ansari and S. Alam, "Hybrid genetic algorithm fuzzy rule based guidance and control for launch vehicle," *In. 11th International Conference on Intelligent Systems Design and Applications, ISDA*, 178–185, 2011.
- [7] M. B. McFarland and S. M. Hoque, "Robustness of a nonlinear missile autopilot designed using dynamic inversion," *In. Proceedings of AIAA Guidance, Navigation, and Control Conference and Exhibit*, 2000.
- [8] D. Ito, D. T. Ward, and J. Valasek, "Robust dynamic inversion controller design and analysis for the X-38," *In. AIAA Guidance, Navigation, and Control Conference and Exhibit*, 2001.
- [9] D. B. Doman and A. D. Ngo, "Dynamic inversion-based adaptive/reconfigurable control of the X-33 on ascent," *Journal of Guidance, Control, and Dynamics*, **25**(2), 275–284, 2002.
- [10] J. O. Pedro, A. Panday, and L. Dala, "A nonlinear dynamic inversion based neurocontroller for unmanned combat aerial vehicles during aerial refuelling," *International Journal of Applied Mathematics and Computer Science*, **23**(1), 75–90, 2013.
- [11] B.I. Adi and T. N. Greville, *Generalized inverses: theory and applications*, Wiley-Interscience Publication, 1974.

- [12] A. H. Bajodah, "Asymptotic perturbed feedback linearisation of underactuated Euler's dynamics," *International Journal of Control*, **82** (10), 1856–1869, 2009.
- [13] A. H. Bajodah, "Generalised dynamic inversion spacecraft control design methodologies," *IET control theory & applications*, **3** (2), 239–251, 2009.
- [14] J. Hall, M. Romano, and R. Cristi, "Quaternion feedback regulator for large angle maneuvers of underactuated spacecraft," *In. American Control Conference*, 2867–2872, 2010.
- [15] A. H. Bajodah, "Asymptotic generalised dynamic inversion attitude control," *IET Control Theory & Applications*, **4** (5), 827–840, 2010.
- [16] I. Hameduddin and A. H. Bajodah, "Nonlinear generalised dynamic inversion for aircraft maneuvering control," *International Journal of Control*, **85** (4), 437–450, 2012.
- [17] H. Gui, L. Jin, and S. Xu, "Attitude control of a rigid spacecraft with one variable-speed control moment gyro," *Acta Mechanica Sinica*, **29** (5), 749–760, 2013.
- [18] H. Gui, L. Jin, and S. Xu, "Attitude maneuver control of a two-wheeled spacecraft with bounded wheel speeds," *Acta Astronautica*, **88**, 98–107, 2013.
- [19] U. Ansari, *Flight vehicle guidance and control*, Masters Thesis, School of Automation Science and Electrical Engineering, Beihang University, 2007.
- [20] X. Yelun, *Rocket Ballistics and Dynamics*, Beijing University of Aeronautics and Astronautics, 2007.
- [21] U. Ansari and A. H. Bajodah, "Generalized dynamic inversion scheme for satellite launch vehicle attitude control," *IFAC-Papers OnLine*, **48** (9), 114–119, 2015.